ELSEVIER

Chemical Engineering Journal 140 (2008) 6–14

Chemical Engineering Journal

www.elsevier.com/locate/cej

Investigations on the kinetics and mechanisms of sorptive removal of fluoride from water using alumina cement granules

S. Ayoob [a], A.K. Gupta [a,*], P.B. Bhakat [a], Venugopal T. Bhat [b]

[a] *Environmental Engineering Division, Department of Civil Engineering, Indian Institute of Technology, Kharagpur 721302, India*
[b] *School of Chemistry, University of Edinburgh, Scotland, UK*

Received 8 April 2007; received in revised form 15 August 2007; accepted 21 August 2007

Abstract

This paper examines the kinetics of fluoride removal from water by the adsorbent alumina cement granules (ALC), exploring the mechanisms involved. ALC exhibited a biphasic kinetic profile of sorption with an initial rapid uptake phase followed by a slow and gradual phase. The kinetic profile has been modeled using pseudo-first-order model, pseudo-second-order model, intraparticle diffusion model and Elovich model. The kinetic sorption profiles offered excellent fit with pseudo-second-order model with a high R^2 value of 0.9987. The value of activation energy of the system (17.67 kJ mol^{-1}) indicates the significance of diffusion in the sorption process. The rate-limiting step of sorption was evaluated by analyzing the response of the system to pH, inert electrolyte concentration, and desorption pattern of the adsorbent, instead of assigning it to a single kinetic model. Accordingly, the surface reactions involving the heterogeneity of the surface site bonding energy or other reactions occurring on the surface of ALC were found predominant in defining the rate-limiting step. The dominant mechanism of fluoride removal appeared to be a chemisorptive ligand exchange reaction involving the formation of inner-sphere complexation of fluoride with ALC.

Keywords: Adsorption; Batch study; Defluoridation; Diffusion; Sorption

1. Introduction

Though low levels of fluoride in water of around 1.0 mg l^{-1} were reported essential in preventing tooth decay [1], its excess presence is of concern due to its human stress effects [2], as is inextricably linked to 'fluorosis'. Among the various technologies developed for defluoridation, adsorption processes are regarded appropriate for the endemic areas of the developing world [3]. Accordingly, the development of socially acceptable, economically viable, and technically feasible robust adsorbents, tailored to meet the local community needs, has become the focus of defluoridation research in the developing world.

One of the most important factors in designing an adsorption system is predicting the rate at which adsorption takes place, referred to the 'kinetics of sorption'. In adsorption processes, the selection of an adsorbent, its configuration, and attainment of equilibrium are related to the 'rate-limiting' process. An understanding of the rate-limiting step will greatly aid in deciding the time of contact to be allowed between the sorbent and sorbate. So, to properly interpret the experimental data, it is necessary to determine the rate-limiting step for the adsorption process, which governs the overall removal rate and mechanisms of sorption. There are essentially three consecutive steps in the adsorption of materials from solution by porous adsorbents, namely bulk diffusion, film diffusion and pore diffusion. Any of these steps can be 'rate-limiting' in adsorption. Generally, both pore diffusion and film diffusion were considered to be the major factors controlling rates of sorption from solution by porous adsorbents. As they act in series, the slower of the two, was regarded as rate-limiting in an adsorption process [4,5].

Recently, exploring on the sorption onto soil-based solid adsorbents, Sparks [6] suggested that the transport processes (non-activated diffusion processes) of sorption include (1) transport in the solution phase (can be eliminated by rapid mixing), (2) transport across a liquid film at the particle/liquid interface (film diffusion) and (3) transport in liquid-filled macropores (>2 nm). The activated diffusion processes include (4) diffusion of a sorbate along pore wall surfaces (surface diffusion), (5) diffusion

* Corresponding author. Tel.: +91 3222 283428; fax: +91 3222 282254.
E-mail addresses: ayoobtkm@yahoo.co.in (S. Ayoob), akgupta@iitkgp.ac.in (A.K. Gupta), phani_jad@yahoo.com (P.B. Bhakat), venu_iitkgp@yahoo.co.in (V.T. Bhat).

1385-8947/$ – see front matter © 2007 Elsevier B.V. All rights reserved.
doi:10.1016/j.cej.2007.08.029

of sorbate occluded in micropores (<2 nm) (pore diffusion) and (6) diffusion processes in the bulk of the solid. The surface and pore diffusion together are referred to as 'interparticle diffusion' while diffusion into the solid adsorbent as 'intraparticle diffusion'.

Sorption reactions can range over a wide time scale (from seconds to years) depending on the nature, availability, and reactivity of sorption sites. Generally, most of the sorption processes exhibits a biphasic uptake with an initial rapid removal phase followed by a slow sorption phase. The rapid step, which occurs over milliseconds to hours, can be ascribed to chemical reactions and film diffusion processes. During this rapid reaction process, a large portion of the sorption may occur. The slow phase which governs the overall rate of sorption could be ascribed to diffusion into micropores, retention on sites of lower reactivity, and surface nucleation/precipitation [6]. Usually, the rate-limiting forces are presumed according to the data fitting to a single kinetic model; commonly, the intraparticle diffusion model by Weber and Morris [7]. However, the kinetic equations that give the best fit are often empirical and the significance of the obtained rate parameters is unclear. So, recent research raises apprehensions over this practice of inferring forces of rate-limiting based only on the fit of kinetics data to a particular model [8]; rather suggest experimental analysis to elucidate the mechanisms.

The three important parameters which may determine the kinetics and rate-limiting process of a sorption system are recently identified as pH, concentration of inert electrolyte, and desorption pattern of the adsorbent [8]. In solutions, the effective particle sizes of the adsorbent are influenced by the concentration of inert electrolyte, with larger aggregated particles being formed in the higher concentrations of inert electrolytes at a given pH. Increasing the effective particle size of the adsorbent will increase the diffusion path length from the external surface of the aggregate to the reactive sites located on its internal surfaces. As a result, it will take a longer time for the ions to reach these reactive sites of the adsorbent from external solution, suggesting rate-limiting.

The adsorbent used in the present study, alumina cement granules (ALC), demonstrated its sorption capacity for removing fluoride from aqueous systems [9]. Since design of a sorption system demands the rate of sorption, this paper focuses on the kinetics of its sorptive responses for process applications. The objectives of this paper are mainly broken down to elucidate (i) the rate-limiting process of sorption and (ii) the mechanisms of fluoride removal.

2. Materials and methods

2.1. Synthesis and characterization of adsorbent

The adsorbent (ALC), selected for the present research, was prepared from commercially available high alumina cement. The rich presence of alumina and calcium, whose (established) potential for fluoride scavenging was instrumental in selection of this adsorbent. Initially, slurry was prepared by adding distilled water to 1 kg of high alumina cement at a water–cement ratio of ~0.3. The slurry was kept at ambient temperature for 2 days for setting, drying and hardening. This hardened paste was cured in water for 5 days. After curing, it was broken, granulated, sieved to geometric mean size of ~0.212 mm, and kept in airtight containers for use.

The elemental composition of ALC (combined with oxygen) was determined by energy dispersive X-ray (EDX) analysis (Oxford ISIS-300 model) by quantitative method in two iterations using ZAF correction, at a system resolution of 65 eV, and results were normalized stoichiometrically. The EDX study showed the presence of Al_2O_3 (78.49%), CaO (15.82%), SiO_2 (5.39%) and Fe_2O_3 (0.30%). The bulk density, specific gravity and pH of zero point charge (pH_{zpc}) were 2.33 g cm^{-3}, 2.587 and 11.32, respectively. The pH at zero point charge of ALC was determined as per the method suggested by Noh and Schwarz [10]. Different quantities of ALC were placed in 10 ml solutions of 0.1 M NaCl (prepared in pre-boiled water) in various bottles and kept in the thermostat shaker for overnight continuous agitation. The equilibrium pH values of these mixtures were measured and limiting value is reported as pH_{zpc}. The surface area of the adsorbent determined by the BET method at liquid nitrogen temperature using FlowSorb II 2300 (Micrometrics Instruments corporation, USA) was found to be 4.385 m^2/g. The chemical composition of ALC was determined by X-ray diffraction analysis (XRD) by Miniflex diffractometer (30 kV, 10 Maq; Rigaku Corp., Tokyo, Japan) with Cu Kα source and a scan rate of 2°/min at room temperature. The Nexus^{TM} 870 spectrometer (Thermo Nicolet) was used for Fourier transform infrared (FTIR) analysis.

2.2. Analyses

All chemicals and reagents used in this study were of reagent-grade and used without further purification. NaF (Merck) was used for preparation of standard fluoride stock solution in double distilled water. All synthetic samples and fluoride solutions for adsorption and analysis were prepared by appropriate dilution of the stock solution in de-ionized (DI) water. Only plastic wares were used for handling fluoride solution and is not prepared in or added to glass containers. All plastic wares were washed in dilute HNO_3 acid bath and rinsed thoroughly with DI water prior to use. Expandable ionAnalyzer EA 940 with Orion ionplus (96-09) fluoride electrode (Thermo Electron Corporation, USA), using TISAB III buffer was used for fluoride measurement. The pH measurement was done by a Cyber Scan 510 pH meter (Oakton Instruments, USA). A temperature-controlled orbital shaker (Remi Instruments Ltd., Mumbai, India) was used for agitation of samples in batch studies. A high precision electrical balance (Mettler Toledo, Model AG135) was used for weight measurement.

2.3. Adsorption and desorption studies

The kinetic and interference tests of fluoride on ALC were carried out in batch system. Polyethylene bottles (Tarson Co. Ltd., India) of 150 ml capacity with 50 ml of fluoride solutions of desired concentration and pH were used. ALC was added as per

dose requirements and bottles were capped tightly and shaken in the orbital shaking incubator at 230 ± 10 rpm. Fluoride samples of desired concentrations were prepared from the stock solution by appropriate dilutions with DI water. All kinetic sorption studies including those at different temperature (290, 300 and 310 K) on equilibrium sorption were conducted with an ALC dose of 2.0 g l^{-1}. The studies on effect of pH, electrolyte concentration, and interference of various ions in synthetic samples were conducted at an ALC dose of 1.5 g l^{-1}. For experiments on pH effects, 2 M HCl or NaOH solutions were added as required. The bottles were taken out from the shaker at desired time intervals and filtered using Whatman no. 42 filter paper to separate the sorbent and filtrate. From the filtered sample of each batch reactor, 10 ml was taken for analysis and determination of residual fluoride. All experiments were duplicated and average values were used for further calculations. In order to check for any adsorption on the walls of the container, blank container adsorption tests were also carried out.

Batch desorption studies were carried out by the dilution method [11] using the spent ALC which has been previously used for fluoride sorption. After completing adsorption up to the equilibrium time of 3 h, 20 ml of the supernatant in the bottle was replaced by equal amount of 10% NaOH. The batch desorption experiments were conducted as per the same experimental procedure followed in adsorption.

The amount of fluoride adsorbed per unit mass of ALC at any time t (q_t, mg g^{-1}), and the adsorption efficiency (%R, determined as the fluoride removal percentage relative to the initial concentration) of the system, was calculated as

$$q_t = \frac{C_0 - C_t}{m} V \quad (1)$$

$$\%R = \frac{C_0 - C_t}{C_0} \times 100 \quad (2)$$

where C_0 and C_t are the fluoride concentrations in solution (mg l^{-1}) initially and at any time (t), respectively, m the mass of ALC (g) and V is the volume (l) of the solution. In Eq. (1), when $C_t = C_e$ (fluoride concentrations remaining in the solution at equilibrium in mg l^{-1}), $q_t = q_e$ (equilibrium adsorption capacity in mg g^{-1}).

3. Results and discussion

3.1. Sorption kinetics

The sorption kinetics indicates the residence time of a sorption reaction as it describes the rate of solute uptake at the solid–solution interface. The sorption of fluoride by ALC exhibited a biphasic uptake as illustrated in Fig. 1. The adsorbent exhibited an initial rapid uptake removing nearly 70% of the initial fluoride concentration within the first 10 min itself. This rapid removal was followed by a slow phase which got stabilized thereafter, with no significant removal after 180 min indicating the attainment of equilibrium. The initial rapid uptake indicates surface bound sorption and precipitative removal, and the slow second phase due to the long-range diffusion of fluoride

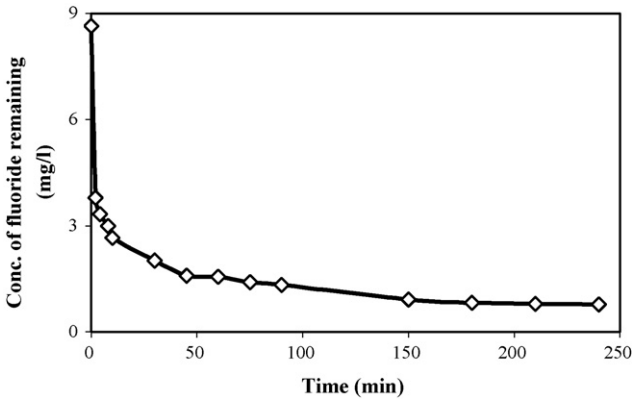

Fig. 1. Sorption of fluoride by ALC with time (Co = 8.65 mg l^{-1}; pH = 6.9 ± 0.4; T = 300 K).

ions onto interior pores of the adsorbent [9,12]. It is generally believed that, when the rate of sorption is rapid, the rate-limiting step is probably a transport process taking place in the liquid phase, such as diffusion in the bulk of the liquid, at the film adjacent to the solid particle, in liquid-filled pores, etc. When the rate of sorption is slow, it is likely that processes taking place at the solid phase are rate determining [13]. Altogether, this slow phase, which denote the rate-limiting step (thereby govern the overall rate of sorption), could be due to diffusion or other surface reactions.

3.2. Kinetic modeling

Based on kinetic data, various models have been suggested which throw light on the mechanisms of sorption and potential rate controlling steps. The models applied to examine the dynamics of the sorption process (represented by Fig. 1) include Lagergren's pseudo-first order, Ho's pseudo-second order, the intraparticle surface diffusion model by Weber and Morris and the Elovich model.

The pseudo-first-order kinetic model based on the solid capacity for sorption analysis by Lagergren is generally expressed as [14,15]:

$$\frac{dq_t}{dt} = k_{s1}(q_e - q_t) \quad (3)$$

Integrating within the boundary conditions $t = 0$ to $t = t$ and $q_t = 0$ to $q_t = q_e$ gives the linearised form as

$$\ln(q_e - q_t) = \ln q_e - k_{s1} t \quad (4)$$

where q_e is the amount of soluted sorbate sorbed at equilibrium (mg g^{-1}), q_t the amount of soluted sorbate on the surface of the sorbent at any time t (mg g^{-1}) and k_{s1} is the pseudo-first-order rate constant (min^{-1}). Based on the linearised form of pseudo-first-order model (Eq. (4)), a linear fit between $\log(q_1 - q_t)$ versus contact time (t) indicate that the reaction may follow a pseudo-first-order. The near linear fits obtained with an R^2 value of 0.975 indicates that the sorption reaction can be approximated to pseudo-first-order kinetics. The pseudo-first-order rate constant k_{s1}, calculated from the slopes of the linear plot was found to be 0.0215 min^{-1}.

If the rate of sorption is a second-order mechanism, the pseudo-second-order chemisorption kinetic rate equation is expressed as [16]:

$$\frac{dq_t}{dt} = k(q_e - q_t)^2 \quad (5)$$

Rearranging and integrating within the boundary conditions $t = 0$ to $t = t$ and $q_t = 0$ to $q_t = q_e$, gives the linearised form as

$$\frac{1}{q_e - q_t} = \frac{1}{q_e} + kt \quad (6)$$

which is the integrated rate law for a pseudo-second-order reaction. Rearranging it again, Eq. (6) reduces to

$$\frac{t}{q_t} = \frac{1}{h} + \frac{1}{q_e}t \quad (7)$$

where k is the pseudo-second-order rate constant ($g\,mg^{-1}\,min^{-1}$) and h is the initial sorption rate ($mg\,g^{-1}\,min^{-1}$), given by

$$h = kq_e^2 \quad (8)$$

where q_e and q_t represents the uptake of fluoride on ALC ($mg\,g^{-1}$) at equilibrium and any time t, respectively. The linear fits obtained according to Eq. (7) showed excellent fit with a very high R^2 value of 0.9987. The low value of k ($0.0625\,g\,mg^{-1}\,min^{-1}$) indicates that the rate of fluoride sorption process is fast.

The concentration dependence of the rate of sorption is commonly used as a partial test of hypothesis regarding the nature of the 'rate-controlling step' and accordingly most of the recent studies involving adsorption of fluoride on metal oxides explored the use of the intraparticle surface diffusion model [17,18] represented by Eq. (9) to elucidate its mechanism [7]:

$$q_t = k_p t^{1/2} + C \quad (9)$$

where k_p is the intraparticle diffusion rate constant and C is a constant related to the thickness of the boundary layer. It was suggested that if the plot of q versus $t^{1/2}$ renders a straight line, intraparticle diffusion controls the sorption process. If it does not pass through the origin, the intraparticle diffusion is not the only rate-limiting step, suggesting that the process is 'complex' with more than one mechanism limiting the rate of sorption. Though the plot of q versus $t^{1/2}$ renders a straight line in the present case ($R^2 = 0.9117$), it fails to pass through the origin [9]. This may also indicate a combined mass transport triggered by initial film mass transfer followed by intraparticle diffusion.

The Elovich equation has also been successfully applied in aqueous systems to describe adsorption and desorption reactions [8,19] as

$$q_t = \frac{1}{\beta}\ln(1 + \alpha\beta t) \quad (10)$$

where α and β are constants, t the time and q_t is the surface coverage. The Elovich equation can be derived from either a diffusion-controlled process or a reaction-controlled process. If the Elovich equation is based on adsorption on an energetically heterogeneous surface, the parameter β is related to the distribution of activation energies. In the diffusion control model, it is a function of particle and diffusion coefficient. When the term $\alpha\beta t$ is much greater than 1, the above equation can be simplified to

$$q_t = \frac{1}{\beta}\ln(\alpha\beta t) = \frac{1}{\beta}\ln(\alpha\beta) + \frac{1}{\beta}\ln(t) \quad (11)$$

The kinetic results will be linear on a q_t versus $\ln t$ plot, if the results follow an Elovich equation. It was suggested that diffusion accounted for the Elovich kinetics pattern [13]; conformation to this equation alone might be taken as evidence that the rate-determining step is diffusion in nature [20]; and that this equation should apply at conditions where desorption rate can be neglected [21]. The kinetic curve of sorption demonstrated excellent fitting with the model ($R^2 = 0.9956$) which may indicate that the diffusional rate-limiting is more prominent in fluoride sorption by ALC. A comparative representation of the kinetics of fluoride sorption data with the applied kinetic models are illustrated in Fig. 2. On comparing the fitting of the applied kinetic models it can be concluded that, the kinetic profile can be best modeled by pseudo-second-order model indicative of a chemisorptive rate-limiting step. Recently, kinetics of many adsorbents in fluoride sorption were well described by pseudo-second-order models [17,22–24].

It was suggested that the value of energy of activation value (E_a), obtained from Arrhenius equation (Eq. (12)) could also be a useful kinetic parameter in assessing rate-limiting steps [6]. Low E_a values usually indicate diffusion-controlled transport and physical adsorption processes, whereas higher E_a values would indicate chemical reaction or surface-controlled processes:

$$K = A_f \exp\left(-\frac{E_a}{RT}\right) \quad (12)$$

where K is the rate coefficient of the sorption reaction ($g\,mg^{-1}\,min^{-1}$), A_f the pre-exponential factor or frequency factor ($g\,mg^{-1}\,min^{-1}$), E_a the activation energy of sorption ($kJ\,mol^{-1}$), R the gas constant ($8.314\,J\,mol^{-1}\,K^{-1}$) and T is the thermodynamic temperature (K). Some of the assigned values of E_a ($kJ\,mol^{-1}$) include 8–25 to physical adsorption, less than 21 to aqueous diffusion, 20–40 to pore diffusion and greater than

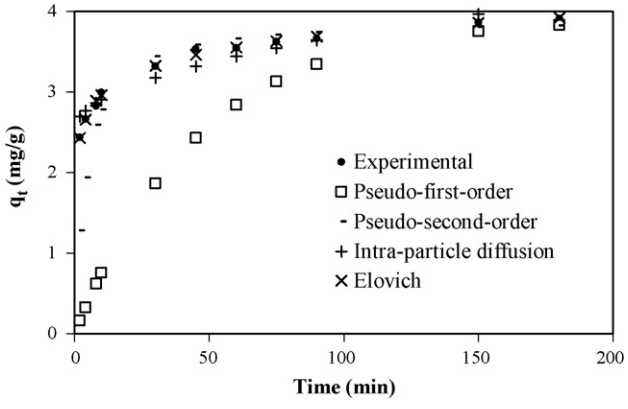

Fig. 2. A comparison of experimental fluoride sorption data with the applied kinetic models ($Co = 8.65\,mg\,l^{-1}$; $pH = 6.9 \pm 0.4$; $T = 300\,K$).

84 to ion exchange. The linear fitting of $\ln K$ versus $1/T$ (graph not shown) rendered an R^2 value of 0.999. The value of E_a was calculated to be 17.67 kJ mol^{-1}. This value of activation energy signifies the role of diffusion-controlled and physical adsorption processes in the rate-limiting of fluoride sorption onto ALC.

3.3. Elucidation of rate-limiting step

The most recent experimental investigations in this direction, comes from Zhang and Stanforth [8]. It was suggested that the slow sorption phase, indicative of the rate-limiting step, may be due to two reasons: (i) diffusion or (ii) surface reactions. As defined earlier, the diffusion may be either interparticle or intraparticle. The surface reactions, includes surface precipitation and surface site bonding energy heterogeneity or other surface reactions. The following procedure was adopted to elucidate the rate-limiting:

(i) If the interparticle diffusion is rate-limiting, then the adsorption patterns should be sensitive to inert electrolyte concentrations or pH.
(ii) If the intraparticle diffusion is rate-limiting, the desorption pattern should follow the same two-stage pattern as that of sorption.
(iii) If both interparticle or intraparticle diffusion are not rate controlling, then by elimination, the surface reactions will be the rate-limiting.

Accordingly, to identify whether it is interparticle diffusion rate-limiting, the effect of pH and electrolyte concentrations were investigated. As demonstrated in Fig. 3, ALC exhibited almost consistent removal potential in the pH range of 3–11.5, getting reduced slightly thereafter by around 10% at pH 12. This pH dependence of fluoride sorption onto ALC could be well explained in terms of its pH_{ZPC} (11.32). The pH_{ZPC} indicates where the net surface charge on the adsorbent is zero. When $pH < pH_{ZPC}$, the net surface charge on solid surface of ALC is positive due to adsorption of excess H^+, which favours adsorption due to coulombic attraction. At $pH > pH_{ZPC}$, the net surface charge is negative due to desorption of H^+ and adsorption must compete with coulombic repulsion. The consistent fluoride removal in the range 3–11.5, could be due to the combined effect of both chemical and electrostatic interactions between the oxide surfaces and fluoride ion. The observed reduction in fluoride adsorption above pH 11.5, may suggest that the strong negative surface charge developed at this pH may cause repulsion for the available adsorption sites. However, the considerable potential of the adsorbent above its pH_{ZPC} of 11.32 may be attributed to the predominance of specific adsorption due to chemical interactions. Similarly, fluoride sorption is found to be unaffected by electrolyte concentrations (Fig. 3) in the range of 10^{-1} to 10^{-4} M $NaNO_3$, though marginal increase was observed at higher concentrations, which may be due to the compression of the electrostatic double layer [25]. The similar findings in fluoride sorption reported for 'lanthanum-exchanged zeolite' were ascribed to the shielding effect [26]. Since the sorption process are unaffected by inert electrolyte concentrations and pH over a wide pH range, it can be suggested that the percentage fluoride removal and hence surface coverage approaches almost the same value within the range of inert electrolyte concentrations tested (10^{-1} to 10^{-4} M), and that rate of sorption is unaffected by effective particle size or diffusive path lengths. This clearly demonstrates that interparticle or external diffusion is not the rate-determining step.

Since the possibility of interparticle or external diffusion is ruled out, the other possibility is that of intraparticle diffusion. As the presence and shape of the pores in an adsorbent does not change with pH or inert electrolyte concentrations, and is only depending on its crystal properties, the desorption behaviour of the adsorbent gives enough indication whether intraparticle diffusion is rate-limiting. If intraparticle diffusion is rate-limiting, it was suggested that, diffusion of the ions out of the pores or the adsorbent during desorption should follow the same two-stage pattern as the diffusion into the pores or adsorbent during its adsorption [8]. However, it was observed in batch desorption studies that concentrations of fluoride increased slowly with time with nearly 52% of the fluoride still not desorbing, and did not reach a steady state even after attaining the equilibrium time of sorption (Fig. 4). The desorption pattern in column studies also showed poor response with much of the fluoride not desorbing with 10% NaOH, even after 20 bed volumes (detailed data

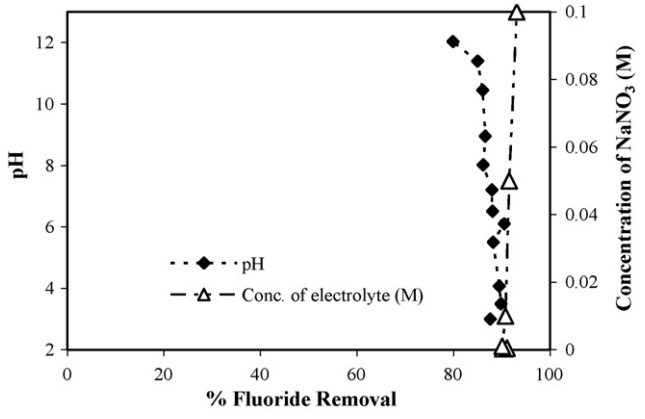

Fig. 3. Effect of pH and inert electrolyte concentrations on the fluoride sorption onto ALC (Co = 8.65 mg l^{-1}; ALC dose = 1.5 g l^{-1}; T = 300 K).

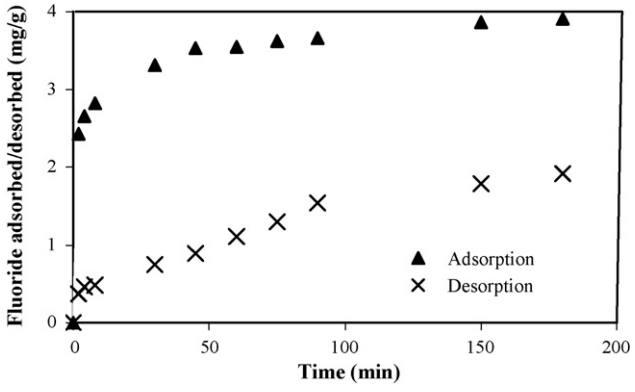

Fig. 4. The sorption and desorption profiles of fluoride onto ALC (Co = 8.65 mg l^{-1}; ALC dose = 2 g l^{-1}; T = 300 K).

not provided). So, it is clear that the adsorption and desorption patterns are not all identical, demonstrating that the diffusion into ALC (i.e. intraparticle diffusion) is not rate-limiting. Since neither interparticle nor intraparticle diffusion is rate-limiting, it indicates that the slow sorption phase in fluoride sorption is not the result of diffusion. So by elimination, it is due either to the heterogeneity of the surface site binding energy or to other reactions controlling fluoride removal from solution.

3.4. Elucidation of fluoride removal mechanisms

Theoretically, there are two widely accepted mechanisms for the adsorption of a solute onto a solid surface. The first one, referred to as the outer-sphere surface complexation (non-specific adsorption) involves electrostatic attraction between a charged surface and an oppositely charged ion in solution. Here, the adsorbed ion resides at a certain distance from the surface. The second one, referred to as the inner-sphere complexation (specific adsorption) involves the formation of a coordinative complex with the solid surface [27]. Since the inner-sphere complex bonds are difficult to break, it results in stronger adsorption of ions than outer-sphere complexes. The chemical evidence of inner-sphere complex formation derives from evaluating the effects of ionic strength and pH on adsorption. Experimental evidences suggest that anions that form inner-sphere complexes coordinate directly with the oxide surface without getting influenced by ionic strength [28]. Since the sorption of fluoride onto ALC is relatively independent of the electrolyte concentrations and pH (Fig. 3) as discussed above, the mechanism of removal can be ascribed to inner-sphere complex formations. Weerasooriya and Wickramarathna [29] also expressed identical views in the adsorption of fluoride by Kaolinite. The poor desorption characteristics of ALC, suggesting stronger adsorption of fluoride ions, further supports the formation of inner-sphere complexes.

The SEM analysis observed Al_2O_3 as the most prominent metal oxide in ALC. Further, the XRD analysis (Fig. 5) carried out to identify the morphological structure and the extent of crystallinity of the adsorbent, shows multiple peaks indicating the presence of various oxides (prominent groups are incorporated in Table 1) indicating heterogeneous surface sites for sorption. So, elucidation of the mechanism is a complex undertaking. Theoretically, upon hydration, the metal ions on the oxide surface

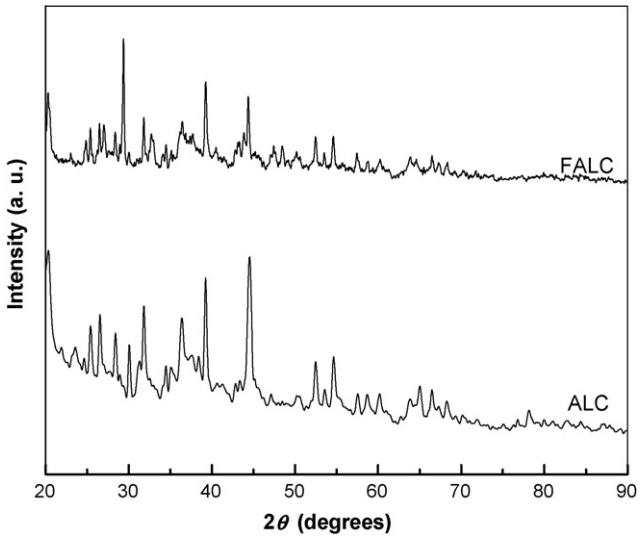

Fig. 5. XRD pattern of the adsorbent before sorption (ALC) and after sorption (FALC).

complete their coordination shells with OH groups. Depending on the pH, these OH groups can bind or release H^+, resulting in the development of a surface charge as

$$MOH + H^+ = MOH_2{}^+ \quad (13)$$

$$MOH = MO^- + H^+ \quad (14)$$

where M represents the metal (Al, Si, Fe, etc.) and $MOH_2{}^+$, MOH and MO^- are positive, neutral and negative surface hydroxo and oxo groups, respectively. Strictly, the adsorption properties of the metal oxides are due to the presence of these $OH_2{}^+$, OH and O^- surface functional groups [30] as it dictates the number of reactive sites. Accordingly, Hao and Huang [31] proposed a surface complex formation model (ligand exchange model) to describe fluoride adsorption on metal oxides as

$$MOH + F^- = MF + OH^- \quad (pH > 7) \quad (15)$$

This equation implies that OH^- is released from the ALC surface into the bulk phase, which is confirmed by the rise in pH during fluoride sorption and was more prominent at initial stages.

To experimentally quantify the process represented by Eq. (15), and to understand spectroscopic changes in the adsorbent (if any) due to fluoride sorption, FTIR analysis were done before

Table 1
Chemical compositions of the adsorbent before sorption of fluoride (ALC) and after sorption on synthetic water (FALC) identified by XRD analysis

ALC		FALC	
Compound name	Chemical formula	Compound name	Chemical formula
Aluminum oxide	Al_2O_3	Fluorite	CaF_2
Aluminum iron silicon	$Al_{0.7}Fe_3Si_{0.3}$	Sodium calcium aluminum fluoride	$NaCa(AlF_6)$
Magnetite	Fe_3O_4	Sodium aluminum fluoride	$NaAlF_4$
Calcium iron oxide	$Ca_4Fe_9O_{17}$	Silicon fluoride	SiF_4
Calcium aluminum oxide	$Ca_3Al_{10}O_{18}$	Villiaumite	NaF
Silicon oxide	SiO_2		
Calcium aluminum silicate	$Ca_{0.88}Al_{1.77}Si_{2.23}O_8$		
Wollastonite	$CaSiO_3$		

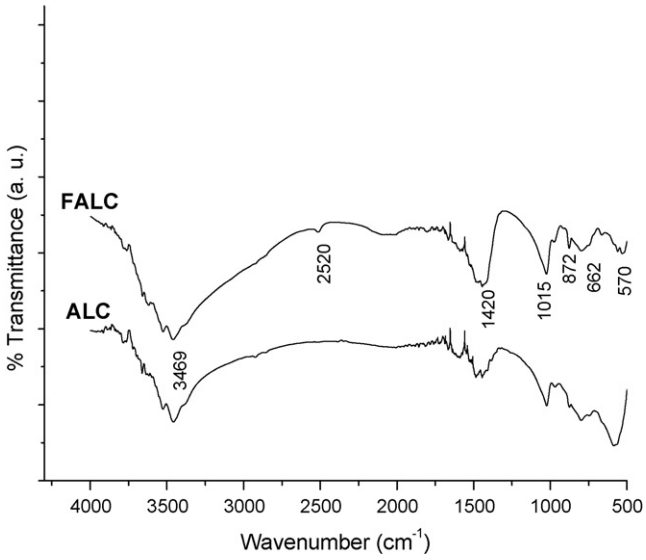

Fig. 6. FTIR spectra of the adsorbent before sorption (ALC) and after sorption (FALC).

and after adsorption. As shown in Fig. 6, the FTIR spectrum of the samples presents no significant spectroscopic change due to fluoride sorption. The broad band corresponding to 3469 cm^{-1} (range of 3550–3200 cm^{-1}) represents O–H stretching vibrations, that at 1420 cm^{-1} to Al–H stretching, and 1015 cm^{-1} represents the characteristic stretching bands of Al=O. The band at 570 cm^{-1} may be ascribed to the stretching of Al–OH, that at 662 cm^{-1} to Si–H and 872 cm^{-1} to Fe–O stretching. On closer examination, it has been observed that the intensity of many of the peaks shows variations after fluoride sorption. Chukin and Malevich [32] demonstrated that the treatment of SiO_2 sample with fluoride results in a decrease in the intensity of the OH^- band at 3750 cm^{-1} or its complete disappearance due to fluoride uptake. This is readily explained, since it is known that OH and F ions have closely similar dimensions and can isomorphously replace each other. So, to ascertain whether such an exchange reaction is taking place in the fluoride sorption onto ALC, the ratio of peak heights of the unbounded surface OH^- band at 3469 cm^{-1} to that at 3750 cm^{-1} are compared before and after adsorption. Before adsorption, in the virgin adsorbent (ALC) this peak height ratio was 1.0256, but after fluoride sorption, it is found to be 2.1348 in the fluoride sorbed adsorbent (FALC). This shows that the OH^- band at 3750 cm^{-1} is decreasing due to fluoride sorption, confirming the exchange of OH ions, enhancing fluoride removal. In the similar way, the peak height ratio of OH^- band at 3469 cm^{-1} to that of Al–OH band at 561 cm^{-1} is also compared. The ratio of the peak height was calculated as 0.99268 in ALC, whereas, it is found to be 2.129 in FALC. This clearly indicates that the OH ions of Al–OH band are consumed in fluoride sorption, more prominently for the exchange reactions with fluoride as represented in Eq. (15). Further, these observations are experimentally supported by the increase in pH observed (6.9 ± 0.4 to 11.7 ± 0.4) due to fluoride uptake especially at the initial stages of sorption. So, the predominant mechanism of fluoride removal can be illustrated as shown in Fig. 7.

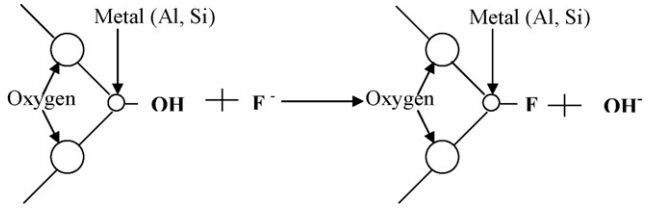

Fig. 7. The ligand exchange model of fluoride sorption onto ALC.

It is also expected that the presence of CaO in ALC may aid in the precipitative removal of fluoride as insoluble CaF_2 ($K_{sp} = 3 \times 10^{-11}$ at 25 °C) as

$$Ca(OH)_2 + 2F^- \rightarrow CaF_2\downarrow + 2OH^- \quad (16)$$

However, the precipitation processes are governed by the solubility of the salt formed. With the value of solubility product for CaF_2 given above, the theoretical minimum fluoride concentration itself amounts to 7.5 mg l^{-1}. Since initial fluoride concentration of the present study is 8.65 mg l^{-1}, precipitation of CaF_2 will occur but may not be considerably high. The results of XRD also support this observation. The formation of aluminum oxide fluoride (Table 1) indicate that chemisorptive sorption is taking place even at higher pH when the net surface of adsorbent is negative [33] in the form of AlO^-. Also it supports the findings that adsorbed fluoride ions remain separated from the surface groups by O or H_2O ligands [29]. The possibility of F adsorption as AlF^{2+} and AlF_2^+ species onto the adsorbent after ligand exchange and co-precipitation was also proposed [34]. But in the present study, the formation of AlF species like sodium calcium aluminum fluoride ($NaCa(AlF_6)$), and sodium aluminum fluoride ($NaAlF_4$) rules out this possibility. The XRD results confirm the mixed surface complex precipitative formations between ions of aluminum, fluoride, hydroxyls, sodium, calcium, iron and silica as suggested by Fletcher et al. [35].

The role of sodium in water (due to NaF addition) deserves special mention, as the reduction in fluoride sorption at high pH may also be attributed to the sodium occupying sorption sites and altering the surface structure. Under basic conditions surface hydronium ions can dissociate allowing the aluminum to serve as a Lewis acid toward cations (like sodium, calcium or iron). This suggests that cations will be sorbed onto the alumina surface under basic conditions. A reaction of this kind, involving the formation of an outer-sphere complex can be expressed as

$$AlOH + Na = AlONa + H^+ \quad (17)$$

Before sodium sorption occurs, =Al–OH and =Al–O^- sites are present in an alkaline solution. The sorption onto alumina (=AlONa) increases under alkaline conditions when the surface of adsorbent is negatively charged [35]. This may lead to electrostatic repulsion between sorbed Na^+ ions and adjacent H^+ ions, causing some H^+ ions break away from the surface and fluoride sorption becomes reduced due to a reduction in available =AlOH sites. So, the concentrations of =Al–OH and =Al–O^- due to sodium occupying sorption sites, in turn reduces the total number of available sites for fluoride sorption. Since these reactions takes place only when the surface charge of ALC is negative,

it indicates that it occurs at the late hours of sorption. This further supports that surface reactions are rate-limiting. Thus the fluoride sorption onto ALC may be viewed as an inner-sphere complexation predominated by a ligand exchange process. The surface reactions leading to mixed surface complex precipitative reactions or scavenging reactions may also be involved.

4. Summary conclusions

The fitting of the kinetic data demonstrate that the dynamics of sorption could be better described by pseudo-second-order model indicating a chemisorptive rate-limiting. XRD reveals multiple oxide surface sites, suggestive of sorption to occur on heterogeneous binding sites. The analysis of FTIR data together with observed increase in pH during sorption suggests that a ligand exchange mechanism is prominent in the removal process. The insensitivity to inert electrolyte concentrations indicates that fluoride may be forming an inner-sphere complex with ALC. It is plausible that the fluoride ions initially attached to ALC by ligand or ion exchange mechanisms may become more firmly bound by chemisorption. The chemical compounds formed due to sorption as indicated by the XRD and the poor desorption characteristics of ALC further demonstrates that such transformations might have taken place. The good fitting of the kinetic data to Elovich and intraparticle diffusion models indicate that diffusion is significant in sorption. The value of activation energy indicates a diffusion-controlled and physical adsorption processes. The poor desorptional characteristics indicate the irreversibility of fluoride sorption, which further suggests that ion exchange is not the only sorption mechanism involved. The response of the system to pH, inert electrolyte concentration and desorption pattern suggest that the slow adsorption phase in fluoride sorption, is not the result of sorption (neither interparticle nor intraparticle); rather the rate-limiting is due either to the heterogeneity of the surface site binding energy or to other reactions controlling fluoride removal from the solution. Overall, the removal of fluoride may be viewed as a complex sorption process, wherein fluoride is 'attached' to ALC through an inner-sphere complex formation through strong bonds (adsorption), diffusion into the crystal structure (absorption), and various surface precipitation reactions.

References

[1] WHO, Fluorides, Environmental Health Criteria, 227, World Health Organization, Geneva, 2002.

[2] S. Ayoob, A.K. Gupta, Fluoride in drinking water: a review on the status and stress effects, Crit. Rev. Environ. Sci. Technol. 36 (2006) 433–487.

[3] R.K. Daw, Experiences with domestic defluoridation in India, in: Proceedings of the 30th WEDC International Conference on People-centred Approaches to Water and Environmental Sanitation, Lao PDR, Vientiane, 2004, pp. 467–473.

[4] D.L. Benefield, J.F. Judkins, B.L. Weand, Process Chemistry for Water and Waste Water Treatment, Prentice-Hall Inc., Englewood Cliffs, NJ, 1982.

[5] W.J. Weber Jr., Adsorption theory, concepts and models, in: F.L. Slejko (Ed.), Adsorption Theory, Marcel Deckker, NY, 1985.

[6] D.L. Sparks, Sorption–desorption, kinetics, in: D. Hillel, J.L. Hatfield, D.S. Powlson, C. Rosenweig, K.M. Scow, M.J. Singer, D.L. Sparks (Eds.), Encyclopedia of Soils in the Environment, Elsevier Ltd., Oxford, UK, 2005, pp. 556–561.

[7] W.J. Weber, J.C. Morris, Kinetics of adsorption on carbon from solution, J. Sanit. Eng. Div. (ASCE) 89 (1963) 31–39.

[8] J. Zhang, R. Stanforth, Slow adsorption reaction between arsenic species and goethite (α-FeOOH): diffusion or heterogeneous surface reaction control, Langmuir 21 (2005) 2895–2901.

[9] S. Ayoob, A.K. Gupta, Sorptive response profile of an adsorbent in the defluoridation of drinking water, Chem. Eng. J. 133 (2007) 273–281.

[10] J.S. Noh, J.A. Schwarz, Estimation of the point of zero charge of simple oxides by mass titration, J. Colloid Interf. Sci. 130 (1989) 157–164.

[11] D.P. Das, J. Das, K. Parida, Physicochemical characterization and adsorption behavior of calcined Zn/Al hydrotalcite-like compound (HTlc) towards removal of fluoride from aqueous solution, J. Colloid Interf. Sci. 261 (2003) 213–220.

[12] J.P. Chen, L. Wang, Characterization of metal adsorption kinetic properties in batch and fixed-bed reactors, Chemosphere 54 (2004) 397–404.

[13] C. Aharoni, D.L. Sparks, S. Levinson, I. Revina, Kinetics of soil chemical reactions: relationships between empirical equations and diffusion models, Soil Sci. Soc. Am. J. 55 (1991) 1307–1312.

[14] S. Lagergren, About theory of so-called adsorption of soluble substances, K. Sven. Ventenskapsakad Handl. 24 (1898) 1–39 (as cited in: Y.S. Ho, G. McKay, A comparison of chemisorption kinetic models applied to pollutant removal on various adsorbents, TransIChemE 76, 332–340).

[15] Y.S. Ho, Citation review of Lagergren kinetic rate equation on adsorption reactions, Scientometrics 59 (2004) 171–177.

[16] Y.S. Ho, G. McKay, Pseudo-second order model for sorption processes, Process Biochem. 34 (1999) 451.

[17] S.M. Maliyekkal, A.K. Sharma, L. Philip, Manganese-oxide-coated alumina: a promising sorbent for defluoridation of water, Water Res. 40 (2006) 3497–3506.

[18] S. Ghorai, K.K. Pant, Equilibrium, kinetics and breakthrough studies for adsorption of fluoride on activated alumina, Sep. Purif. Technol. 42 (2005) 265–271.

[19] F.J. Hingston, in: M.A. Anderson, A.J. Rubin (Eds.), Adsorption of Inorganics at the Solid–Liquid Interface, Ann Arbor Science, Ann Arbor, MI, 1981, p. 67.

[20] A. Pavlatou, N.A. Polyzopouls, The role of diffusion in the kinetics of phosphate desorption: the relevance of the Elovich equation, Eur. J. Soil Sci. 39 (1988) 425–436.

[21] W. Rudzinksi, P. Panczyk, in: J.A. Schwarz, C.I. Contescu (Eds.), Surfaces of Nanoparticles and Porous Materials, Dekker, New York, 1998, p. 355.

[22] S.V. Ramanaiah, S. Venkata Mohan, P.N. SarmaRamanaiah, Adsorptive removal of fluoride from aqueous phase using waste fungus (*Pleurotus ostreatus* 1804) biosorbent: kinetics evaluation, Ecol. Eng. 31 (2007) 47–56.

[23] R. Sai Sathish, S. Sairam, V. Guru Raja, G. Nageswara Rao, K. Anil Kumar, C. Janardhana, Kinetics and adsorption characteristics of fluoride on zirconium impregnated coconut fiber carbon, J. Fluorine Chem. (2007), doi:10.1016/j.jfluchem.2007.06.002.

[24] S.P. Kamble, S. Jagtap, N.K. Labhsetwar, D. Thakare, S. Godfrey, S. Devotta, S.S. Rayalu, Defluoridation of drinking water using chitin, chitosan and lanthanum-modified chitosan, Chem. Eng. J. 129 (2007) 173–180.

[25] J.P. Chen, M.S. Lin, Equilibrium and kinetic of metal ion adsorption onto a commercial h-type granular activated carbon: experimental and modeling studies, Water Res. 35 (2001) 2385–2394.

[26] S.M. Onyango, Y. Kojima, O. Aoyi, C.E. Bernardo, H. Matsuda, Adsorption equilibrium modeling and solution chemistry dependence of fluoride removal from water by trivalent-cation-exchanged zeolite F-9, J. Colloid Interf. Sci. 279 (2004) 341–350.

[27] F.J. Hingston, A.M. Posner, J.P. Quirk, Anion adsorption by goethite and gibbsite. I. The role of proton in determining adsorption envelops, J. Soil Sci. 23 (1972) 177–192.

[28] K.G. Stollenwerk, Geochemical processes controlling transport of arsenic in ground water: a review of adsorption, in: A.H. Welch, K.G. Stollenwerk (Eds.), Arsenic in Ground Water, Kluwer Academic Publishers, Boston, 2003, pp. 67–100.

[29] R. Weerasooriya, H.U.S. Wickramarathna, Modeling anion adsorption on kaolinite, J. Colloid Interf. Sci. 213 (1999) 395–399.
[30] G. Sposito, The Surface Chemistry of Soils, Oxford University Press, 1984, p. 234.
[31] J.O. Hao, C.P. Huang, Adsorption characteristics of fluoride onto hydrous alumina, J. Environ. Eng. (ASCE) 112 (1986) 1054–1067.
[32] G.D. Chukin, V.I. Malevich, Infrared spectra of silica, J. Appl. Spectrosc. 26 (1977) 294–301.
[33] A.L. Valdivieso, J.L.R. Bahena, S. Song, R.H. Urbina, Temperature effect on the zeta potential and fluoride adsorption at the α-Al_2O_3/aqueous solution interface, J. Colloid Interf. Sci. 298 (2006) 1–5.
[34] M.X. Zhu, M. Xie, X. Jiang, Interaction of fluoride with hydroxyaluminum–montmorillonite complexes and implications for fluoride-contaminated acidic soils, Appl. Geochem. 21 (2006) 675–683.
[35] H.R. Fletcher, D.W. Smith, P. Pivonka, Modeling the sorption of fluoride onto alumina, J. Environ. Eng. (ASCE) 132 (2006) 229–246.